Journal of Engineering and Applied Sciences 13 (23): 9985-9993, 2018
ISSN: 1816-949X

PSD Calculations of the Intrachannel Nonlinearity Distortion Using Quantum Description for M-QAM-Square Techniques

[1]Mahdi Zaman, [1]Ali Hadi Hassan Al-Batat and [2]Hassan Abid Yasser
[1]Department of Physics, College of Education, Mustansiriyah University,
P.O. Box: 46219 Baghdad, Iraq
[2]Department of Physics, College of Science, Thi-Qar University, Thi-Qar, Iraq

Abstract: In highly dispersive single-channel fiber, the optical signal propagation within channel leads to significant signal broadening and thereby, it interacts nonlinearly with a large number of neighboring signals. The overlap-states leads to create echo signals in "0" bit slots and amplitude jitter in "1" bits slots too that can significant limit the system performance due to increasing in a Bit Error Rate (BER). In this thesis, the Power Spectral Density (PSD) of the intrachannel nonlinearity distortion of a chirped Gaussian pulses is investigated theoretically using the small perturbation technique and the statistical quantum description of square M-QAM systems. Additionally, we provided an analytical expression using the perturbation coefficient matrix $\tilde{X}_{lmn}(\omega)$ of PSD to estimate a Signal to Noise Ratio (SNR). We assumed that the noise is Additive White Gaussian Noise (AWGN) and all transmitted signals undergo equal probability of distribution on coherent receiver where MATLAB programming are used to check out validity of analytical model. Our simulation shows that the intrachannel distortion is mitigated significantly by choosing of initial suitable parameters. Consequently, improving the SNR to acceptable values is achieved.

Key words: Intrachannel nonlinearity, Power Spectral Density (PSD), M-QAM square systems, parameters, Gaussian pulses, intrachannel

INTRODUCTION

In a highly dispersive fiber with high-speed systems at 40 GB/sec and above, the signal broadens significantly and thereby, it interacts nonlinearly with a large number of neighboring signals. In the time domain, this means that the spectral components overlap with different phases in a certain time. However, the signals overlapping in coherent optical communications creates nonlinear restriction such as intrachannel interactions such Intrachannel Self-Phase Modulation (ISPM), intrachannel cross-phase modulation IXPM and Intrachannel Four Wave Mixing (IFWM). The ISPM-induced by nonlinear phase noise and the IXPM-induced by timing jitter (or broadening) in the "1" time slots while the IFWM-induced by echo pulses in the "0" time slots and amplitude jitter in the "1" time slots resulting from energy transfer among signals within the same wavelength channel (Djordjevic and Vasic, 2006). Furthermore, the statistical characteristic of received bits is a fundamental concern in communication systems. Because of the highly fiber nonlinearity in long-haul fiber-optic communication systems, it is usually hard to obtain the exact analytical expression for the PSD of received bits which is translated to timing delay because of dispersion (Tao *et al*., 2015). However, in spite of they were very helpful for increasing of information transmitted capacity, the previous studies on the statistical characteristics of nonlinear noise, i.e., spectrum and power pulses, it is not sufficient for nonlinear compensation (Bononi *et al*., 2011). Nonlinear compensation requires the capability to calculate the nonlinear noise waveform. Consequently, the modeling of intrachannel nonlinear distortion in coherent fiber-optic systems on QAM has drawn significant research interest (Gnauck *et al*., 2012).

By Naderi (2013), analytical expressions of PSD of intrachannel nonlinear distortion using a first order perturbation theory is derived based on QPSK and 16 QAM techniques. By Liang (2015) analytical expressions of PSD and compensations of intrachannel nonlinear distortion in Wavelength Division Multiplexing (WDM) systems. In this study, we checked out the impact of chirp parameter on the intrachannel nonlinearity impairments for square M-QAM transmission systems using statistical model. The simulation is executed by MATLAB programming.

Corresponding Author: Mahdi Zaman, Department of Physics, College of Education, Mustansiriyah University,
P.O. Box: 46219 Baghdad, Iraq

MATERIALS AND METHODS

Perturbed nonlinear Schrodinger equation: The Nonlinear Schrodinger Equation (NLSE) for an initial pulse duration T_0>5 ps in single-mode fiber is:

$$\frac{\partial u}{\partial z}+i\frac{\beta_2}{2}\frac{\partial^2 u}{\partial t^2}=i\gamma(z)|u|^2u \quad (1)$$

Where:

$\gamma(z)=\gamma_0 e^{-\int_0^z \alpha(z')dz'}$ = The nonlinear coefficient
β_2 = The second order dispersion parameter
αz = The fiber attenuation coefficient

For interacted pulses transmit through a multi span link with perfect dispersion compensation per span, the electric field can be decomposed as a sum of fields of individual pulses:

$$u(z,t)=\sqrt{P_0}\sum_{n=-\infty}^{\infty}a_n f(t-nT_b) \quad (2)$$

Where:

P_0 = The peak power
nT_b = The symbol bit interval
n = The position of bit
a_n = The random variables depending on modulation technique
$f(t-nT_b)$ = The pulse profile shape (Shake *et al*., 1998)

Considering as a small perturbation, the analytical analysis of nonlinearity effect is:

$$u(z,t)=\sum_{n=-\infty}^{\infty}a_n u_n+\Delta u \quad (3)$$

Where:

Δu = The perturbation due to Kerr nonlinearity
u_n = The linear solution to the NLSE

Let's consider serial bits of chirped pulse, the linear solution is (Agrawal, 2012):

$$u(z,t)=\frac{T_0\sqrt{P_0}}{T}\sum_n a_n\exp\left[-\frac{1+iC}{2}\frac{(t-nT_b)^2}{T^2}\right] \quad (4)$$

Where:

T^2 = T_0^2-iD(1+iC)
T_0 = The initial pulse-width
C = The initial input chirp

and $D(z)=\int_0^z \beta_2 dz'$ is the dispersion over a period z. By substituting Eq. 3 in Eq. 1 through (Eq. 4), the modified perturbation NLSE will has the form:

$$\frac{\partial \Delta u}{\partial z}+i\frac{\beta_2}{2}\frac{\partial^2 \Delta u}{\partial t^2}=i\gamma(z)$$
$$\sum_{l,m,n=-s}^{s}a_l a_m a_n^* u_l u_m u_n^*=iF(z,t) \quad (5)$$

where, l, m and n are the interacted pulses locations. Here, we assume intrachannel nonlinearity as contribution of neighboring bits on both sides of central bit, i.e., (l, m, n)$\in$[-s, s]. The right-hand side of Eq. 5 represents effects of intrachannel nonlinearity which may be identified as follows: the case l = m = n corresponds to ISPM, the case l = n.m or l.n = m or l.n = m to IXPM and the case l = m.n to degenerate IFWM and l.m.n to non-degenerate IFWM (Hirooka and Nakazawa, 2015). The variance between the input and output signals is obtained by solving the differential Eq. 5 as:

$$\Delta\tilde{u}(L_{tot},\omega)=i\int_0^{L_{tot}}\tilde{F}(z,\omega)\exp\left[-iD(z)\omega^2/2\right]dz \quad (6)$$

Where:

L_{tot} = The total transmission distance
$\tilde{F}(z,\omega)$ = The Fourier transform of F(z, t) that is given by appendix A)

The forcing function F(z, t) in Eq. 5 can be written as:

$$F(z,t)=\frac{\gamma(z)P_0^{3/2}T_0^3}{|T|^2T}\sum_{l,m,n=-s}^{s}a_l a_m a_n^* r_l r_m r_n^* \quad (7)$$

By rearranging Eq. 45, for centered echo pulse at t = 0, we have special case parameters:

$$F(z,t)=\frac{\gamma(z)\bar{P}_0^{3}T_0^3}{|T|^2T}\sum_{l,m,n=-s}^{s}a_l a_m a_n^* e^{-\varepsilon_1 t^2+\varepsilon_2 t-\varepsilon_3} \quad (8)$$

Where:

$$\varepsilon_1=\frac{3T_0^2+iK}{2\left[\left(T_0^2+DC\right)^2+D^2\right]} \quad (9)$$

$$\varepsilon_2=\frac{(\varepsilon_4)^2}{4\varepsilon_1}\left(1-\frac{1}{1+2i\varepsilon_1 D}\right) \quad (10)$$

$$\varepsilon_3=\frac{T_0^2\left[\left(l^2+m^2\right)+ml(1-iK/T_0^2)\right]T_b^2}{\left[\left(T_0^2+DC\right)^2+D^2\right]} \quad (11)$$

$$\varepsilon_4=\frac{2T_0^2(l+m)T_b}{\left[\left(T_0^2+DC\right)^2+D^2\right]} \quad (12)$$

And:

$$K = D+C\left(T_0^2+DC\right) \quad (13)$$

Taking Fourier transform of Eq. 46 to get:

$$\tilde{F}(z,\omega) = \frac{\gamma(z)P_0^{\frac{3}{2}}T_0^3}{|T|^2 T}\sqrt{\frac{p}{\varepsilon_1(z)}}\sum_{l,m,n=-s}^{S} a_l a_m a_n^* e^{-\varepsilon_3(z)+\frac{\left[\varepsilon_2(z)+i\omega\right]^2}{4\varepsilon_1(z)}} \quad (14)$$

where, we use the identity:

$$\int_{-\infty}^{+\infty} e^{-(ax^2-bx+c)}dx = \sqrt{\frac{\pi}{a}}e^{\frac{b^2}{4a}-c} \quad (15)$$

$$\tilde{F}(z,\omega) = \frac{\gamma(z)P_0^{\frac{3}{2}}T_0^3}{|T|^2 T}\sqrt{\frac{p}{E_1(z)}}\sum_{l,m,n=-s}^{s} a_l a_m a_n^* e^{-\varepsilon_3(z)+\frac{\left[\varepsilon_2(z)+i\omega\right]^2}{4\varepsilon_1(z)}} \quad (16)$$

PSD of nonlinear intrachannel distortion: For echo pulse has a Gaussian distribution centered at (l+m-n = j), j,[-s, s], Eq. 6 can be rearranged as follows:

$$\Delta\tilde{u}(L_{tot},\omega) = \gamma_0 P_0^{\frac{3}{2}}\sum_{l,m,n=-s}^{s} a_l a_m a_n^* \tilde{X}_{lmn}(\omega) \quad (17)$$

Where:

$$\tilde{X}_{lmn}(\omega) = i\int_0^{L_{tot}} G e^{p\omega^2+q\omega+r}dz \quad (18)$$

$$p = \frac{iD}{2}-\frac{1}{4\varepsilon_1} \quad (19)$$

$$q = \frac{i\varepsilon_2}{2\varepsilon_1} \quad (20)$$

$$r = -\alpha z-\varepsilon_3+\frac{(\varepsilon_2)^2}{4\varepsilon_1} \quad (21)$$

and

$$G = \frac{T_0^3\pi^{1/2}}{|T|^2 T(\varepsilon_2)^{1/2}} \quad (22)$$

The PSD of the nonlinear distortion is define as (Kahn and Ho, 2004):

$$\rho_{NL}(\omega) = \lim_{s\to\infty}\frac{1}{(2s+1)T_b}\left\langle\left|\Delta\tilde{u}(\omega)\right|^2\right\rangle \quad (23)$$

Substituting Eq. 8 in Eq. 10 to obtain:

$$\rho_{NL}(\omega) = \lim_{s\to\infty}\frac{\gamma_0^2 P_0^3}{(2s+1)T_b}\sum_{l,m,n,l',m',n'=-s}^{s} \left\langle a_l a_m a_n^* a_{l'}^* a_{m'}^* a_{n'}\right\rangle \times \tilde{X}_{lmn}(\omega)\tilde{X}_{l'm'n'}^*(\omega) \quad (24)$$

By choosing an intersymbol interference-free sampling pulse at $t = nT_b$, the nonlinear PSD can be divided into six groups depend on the state of variables (l, m, n, l', m', n'). They are ND-IFWM, D-IFWM), ISPM, IXPM, D-IFWM and ND-IFWM correlation and ISPM and IXPM correlation (Naderi, 2013).

Quantum description for square M-QAM techniques: In the information transmission systems, the received signal is random due to the random arrival time of photons. This is not a flaw in the detector but rather is a fundamental law of physics as dictated by quantum mechanics. Theoverlapping states in quantum mechanics is a specific kind of quantum state that is an equivalent of a classical monochromatic electromagnetic wave. In M-QAM system, each amplitude of the signal can be calculated by factor 2^z as:

$$M = 2^z,\ z\in\square \quad (25)$$

In general case, for even values of z, the constellations are square (4-QAM, 16-QAM, 64-QAM, ..., M-QAM). However, using completeness relation, the signal quantum state for square M-QAM denoted by a random variable quantity can be defined as a set of a linear combination:

$$\left|a_n\right\rangle = \sum_{x,y} c_{x,y}\left|a_{x,y}\right\rangle \quad (26)$$

where $|a_{x,y}$ stands for a partial probability of signal quantum state or the overlapping states light having complex amplitude, $a_{x,y}$, $c_{x,y}$ is a partial probability amplitude of linear combination, x = ±1, ±3, ..., X and y = ±1, ±3, ..., Y. For square M-QAM, both $x, Y = \pm\left(\sqrt{M}-1\right)$ where, $\sqrt{M}\in z$ is the number of amplitude levels of in-phase and quadrature components, respectively (Kato, 2012). In case of X, Y = 2 or index set {±1}, we obtain 4-QAM format. In case of index set {±1, ±3}, we obtain 16-QAM format. In case of index set {±1, ±3, ±7}, we obtain 64-QAM format. At the last, in the case of index set {±1, ±3, ±7, ±15}, we obtain 256-QAM format.

When we use the geometric criterion, the overlapping states $|a_{x,y}$ can be denoted as signal overlapping states $|a_m$ and the partial probability amplitude $c_{x,y}$ can be denoted as the partial probability amplitude c_m where, m = 1, 2, …, M. So, the signal 256-QAM (e.g.,) is defined as of overlapping states as follow (Chen *et al*., 2015):

$$\left|a_n\right\rangle c_1\left|a_1\right\rangle+c_2\left|a_2\right\rangle+, ..., +c_M\left|a_M\right\rangle \quad (27)$$

Where:

$$\begin{aligned}|a_1\rangle &= |A(-15\text{-}15i)\rangle\\ |a_2\rangle &= |A(-15\text{-}7i)\rangle\\ |a_3\rangle &= |A(-15\text{-}3i)\rangle\\ &\vdots\\ |a_{256}\rangle &= |A(15+15i)\rangle\end{aligned} \tag{28}$$

$A = 1/\sqrt{2}$ is a real valued fundamental amplitude while Euclidian distance between first order neighboring states or the minimum signal distance is 2A (Kato, 2012). Thus, the average number of photons of overlapping states corresponding to degeneration degree, N_g is defined:

$$N_g = \sum_{m=1}^{M} P_m |a_m|^{2g},\ g = 1, 2, 3 \tag{29}$$

where, P_m is a priori probabilities of quantum states density (Chen *et al*., 2015). To simplify the calculations, we have to focus on the equal probability case, that is $P_m = |c_m|^2 = 1/M$ for all m where the total priori probability of signal satisfy completeness principle:

$$\sum_{m=1}^{M} P_m = 1,\ P_m \geq 0 \tag{30}$$

By using Eq. 16, we found N_1-N_3 values for four types of square M-QAM illustrated in Table 1. These values are very important to calculate the PSD of difference types of intrachannel nonlinear impairments.

PSD calculation: To determine the total PSD results from intrachannel nonlinearity, we have to consider each effect separately.

PSD of IFWM: Using Eq. 11, we obtain to general equation that describe the PSD due to ND-IFWM as:

$$\rho_{\text{ND-IFWM}}(\omega) = \lim_{s\to\infty} \frac{2N_1^3\gamma_0^2P_0^3}{(2s+1)T_b} \sum_{l,\,m,\,n=-s}^{s} \left|\tilde{X}_{lmn}(\omega)\right|^2 \tag{31}$$

Eq. 18 can be rewritten as follows:

$$\rho_{\text{ND-IFWM}}(\omega) = \lim_{s\to\infty} \frac{2N_1^3\gamma_0^2P_0^3}{(2s+1)T_b} \left\{ \sum_{l\neq m,\, l+m-n=-s} \sum_{m} \sum_{n} |\tilde{X}_{lmn}(\omega)|^2 + \sum_{l\neq m,\, l+m-n=-s+1} \sum_{m} \sum_{n} |\tilde{X}_{lmn}(\omega)|^2 + ,\ldots, + \sum_{l\neq m,\, l+m-n=s} \sum_{m} \sum_{n} |\tilde{X}_{lmn}(\omega)|^2 \right\} \tag{32}$$

The jth term on the right-hand side RHS of Eq. 19 represents the nonlinear distortion on the jth symbol interval. A symmetry around centered echo pulse leads to make the average of the nonlinear distortion should be the same on each symbol interval. In the other words, each term on the RHS of Eq. 19 should be equal which yields to:

Table 1: Values of N_1-N_3 for various types of square M-QAM

Modulation techniques	N_1	N_2	N_3
4 QAM	1	1	1
16 QAM	5	33	245
64 QAM	21	609	20613
256 QAM	85	10081	1407685

$$\rho_{\text{ND-IFWM}}(\omega) = \frac{2N_1^3\gamma_0^2P_0^3}{T_b} \sum_{l\neq m,\, l+m-n=0} |\tilde{X}_{lmn}(\omega)|^2 \tag{33}$$

Using the characteristics of autocorrelation, the PSD due to D-IFWM will be:

$$\rho_{\text{D-IFWM}}(\omega) = \lim_{s\to\infty} \frac{N_1N_2\gamma_0^2P_0^3}{(2s+1)T_b} \left\{ \sum_{l=m,\, l+m-n=-s} \sum_{l} \sum_{n} |\tilde{X}_{lln}(\omega)|^2 + \sum_{l=m,\, l+m-n=-s+1} \sum_{l} \sum_{n} |\tilde{X}_{lln}(\omega)|^2 + ,\ldots, + \sum_{l=m,\, l+m-n=s} \sum_{l} \sum_{n} |\tilde{X}_{lln}(\omega)|^2 \right\} \tag{34}$$

Proceeding as before, leads to:

$$\rho_{\text{D-IFWM}}(\omega) = \frac{N_1N_2\gamma_0^2P_0^3}{T_b} \sum_{2l=n} \left|\tilde{X}_{lln}(\omega)\right|^2 \tag{35}$$

PSD of ISPM and IXPM: Since, both have phase-independent distortions, conclusion is that both the ISPM and ISPM are correlated. Considering only the ISPM and IXPM, we have:

$$\Delta\tilde{u}(L_{tot}, \omega) \equiv \Delta\tilde{u}_{PM}(\omega) = \Delta\tilde{u}_{ISPM} + \Delta\tilde{u}_{IXPM} \tag{36}$$

Where:

$$\Delta\tilde{u}_{ISPM} = \gamma_0 P_0^{\frac{3}{2}} \sum_{l=-s}^{} |a_l|^2 a_l \tilde{X}_{lmn}(\omega) \tag{37}$$

And:

$$\Delta\tilde{u}_{IXPM} = \gamma_0 P_0^{\frac{3}{2}} \sum_{l,\, m=-s,\, l\neq m} |a_m|^2 a_l \tilde{X}_{lmn}(\omega) \tag{38}$$

The PSD due to SPM and IXPM is:

$$\rho_{PM}(\omega) = \lim_{s\to\infty} \frac{\left\langle \left|\Delta\tilde{u}_{PM}(\omega)\right|^2 \right\rangle}{(2s+1)T_b} = \rho_{ISPM}(\omega) + \rho_{IXPM}(\omega) + \rho_{ISPM\text{-}IXPM}(\omega) \tag{39}$$

The contribution of PSD due to ISPM can be accounted using autocorrelation characteristics and Eq. 24:

$$\rho_{ISPM}(\omega)=\frac{N_3\gamma_0^2P_0^3}{T_b}\sum_{l=-s}^{s}\left|\tilde{X}_{lll}(\omega)\right|^2 \quad (40)$$

$$=\frac{N_3\gamma_0^2P_0^3}{T_b}\left|\tilde{X}_{000}(\omega)\right|^2 \quad (41)$$

Using characteristics of autocorrelation, the contribution of PSD due to IXPM is:

$$\rho_{IXPM}(\omega)=\lim_{s\to\infty}\frac{2\gamma_0^2P_0^3}{(2s+1)T_b}\sum_{l,\,m,\,n'=-s}^{s}N_1N_{mn'}\tilde{X}_{lmm}(\omega)\tilde{X}^*_{ln'n'}(\omega) \quad (42)$$

$$\frac{2\gamma_0^2P_0^3}{T_b}\left\{N_1N_2\sum_{m\neq0,\,m=-s}^{s}\left|\tilde{X}_{0mm}(\omega)\right|^2+N_1^3\sum_{m\neq n',\,m\neq0,\,n'\neq0,\,m,\,n,\,n'=-s}^{s}\tilde{X}_{0mm}(\omega)\tilde{X}^*_{0n'n'}(\omega)\right\} \quad (43)$$

The contribution to the PSD due to the correlation between ISPM and IXPM is:

$$\rho_{ISPM-IXPM}(\omega)=\lim_{s\to\infty}\frac{2N_1N_2\gamma_0^2P_0^3}{(2s+1)T_b}\sum_{l,\,n'=-s}^{s}\tilde{X}_{lll}(\omega)\tilde{X}^*_{ln'n'}(\omega) \quad (44)$$

$$\frac{2N_1N_2\gamma_0^2P_0^3}{T_b}\sum_{n\neq0,\,n=-s}^{s}\tilde{X}_{000}(\omega)\tilde{X}^*_{0nn}(\omega) \quad (45)$$

Total PSD and variance calculations: Combining Eq. 20, 21 and 26, the nonlinear PSD will be:

$$\rho_{NL}(\omega)=\rho_{ND-IFWM}(\omega)+\rho_{D-IFWM}(\omega)+\rho_{PM}(\omega) \quad (46)$$

Equation 33 estimates the nonlinear PSD for a chirped Gaussian pulses propagation in single-channel fiber based on square M-ray QAM. The main result is that $\rho_{NL}(\omega)$ increases significantly with an increasing of M-QAM order, due to directly proportional with values of N_1-N_3.

Channel capacity limit calculations quantifying the effects of fiber nonlinearity can be plausibly represented as statistically independent AWGN, the variance of which may be added to that of ASE (Zhang *et al*., 2017). Consequently, by ignoring the interplay between the amplifier noise and nonlinearity (so called Gordon-Mollenauer noise), the total PSD is given by:

$$\rho_{tot}(\omega)=\rho_{NL}(\omega)+\rho_{ASE}(\omega) \quad (47)$$

where $\rho_{ASE}(\omega)$ is the spectral density of amplified spontaneous emission that is given by:

$$\rho_{ASE}(\omega)=\frac{1}{2\pi}\sum_{j=1}^{NA}\left(e^{\alpha L_{a,j}}-1\right)h\bar{\omega}n_{sp} \quad (48)$$

Where:

N_A = Number of amplifiers
$L_{a,j}$ = Amplifier's spacing
h = Planck constant
$\bar{\omega}$ = The mean frequency of the channel
n_{sp} = Spontaneous noise factor

Gaussian pulses filtering: Noise reduction is a key step for digital signal processing due to the presence of the high noise levels in the signal pulses for a high bit communication systems. Filters based on Gaussian functions are of particular importance because their shapes are easily specified and both the forward and inverse Fourier transforms of a Gaussian function are real Gaussian functions. Whether in spatial domain or in frequency domain, Gaussian smoothing filter is a kind of effective low-pass filter, especially to remove the noises that are subject to the normal distribution (Jain and Gupta, 2015). The Gaussian filter is given by Wang *et al*. (2014):

$$h(t)=\frac{1}{\sqrt{2p}}\exp\left(-\frac{t^2}{2\eta^2T_b^2}\right) \quad (49)$$

where, ηT_b is standard deviation of Gaussian distribution which satisfy the following defnition:

$$\eta T_b=\frac{\sqrt{\ln 2}}{2\pi B} \quad (50)$$

Now, take Fourier transformation of Eq. 36 to estimate the received signal variance:

$$\tilde{H}(\omega)=\eta T_b\exp\left(-\frac{\eta^2T_b^2\omega^2}{2}\right) \quad (51)$$

Using the Wiener-Khinchin theorem, the total variance is:

$$\sigma_{tot}^2=\frac{1}{2\pi}\int_{-\infty}^{+\infty}\rho_{tot}(\omega)\left|\tilde{H}(\omega)\right|^2d\omega \quad (52)$$

$$\frac{1}{2\pi}\int_{-\infty}^{+\infty}\rho_{tot}(\omega)\delta^2T_b^2\exp\left(-\delta^2T_b^2\omega^2\right)d\omega \quad (53)$$

The integral of Eq. 40 will be within range-bandwidth [-B, B].

SNR and probability error calculations: Calculations of SNR are generated by averaging observable properties of the received signal over a number of symbols. If a matched filter is employed at the receiver, the SNR as

defined here is related to the ratio of the bit energy-to-noise power spectral density per symbol (Zhang *et al*., 2017):

$$SNR = \frac{P_0}{1.88\sigma_{tot}^2} \tag{54}$$

The exact expression of average bit -error probability of square M-QAM can be obtained by averaging the bit error probability of the kth bit, $P_{b(k)}$ (Cho and Yoon, 2002):

$$P_b = \frac{1}{\log_2\sqrt{M}} \sum_{k=1}^{\log_2\sqrt{m}} P_b(k) \tag{55}$$

where $k \in \{1, 2, ..., \log_2\sqrt{m}\}$. The $P_b(k)$ that the kth bit is in error, characterizes the BER of square M-QAM scheme is expressed as (Lopes *et al*., 2007; Schmidt *et al*., 2016):

$$P_b(k) = \frac{1}{\sqrt{M}} \sum_{i=0}^{(1-2^{-k})\sqrt{M}-1} \left\{ (-1)^{\left\lfloor \frac{i.2^{k-1}}{\sqrt{M}} \right\rfloor} .2^{k-1} - \left[\frac{i.2^{k-1}}{\sqrt{M}} + \frac{1}{2} \right] .\text{erfc}\left((2i+1)\sqrt{\frac{3SNR}{2(M-1)}} \right) \right\} \tag{56}$$

where $\lfloor x \rfloor$ denotes the largest integer smaller than x and erfc (x) denotes as the complementary error function that is given by:

$$\text{erfc}(x) = \frac{2}{\sqrt{\pi}} \int_x^\infty e^{-\tau^2} d\tau \tag{57}$$

RESULTS AND DISCUSSION

For M-QAM square transmission techniques, calculations of nonlinear variance induced by AWGN in single-core channel with dispersion compensation at receiver are carried out using simulation of Eq. 40. On the other hand, SNR and BER are obtained by Eq. 41 and 42, respectively. The simulation is done using self-developed MATLAB programming.

In our calculations, we ignored all addition noise as ASE noise. Unless otherwise specified, the parameters mentioned in caption of each figure (Table 2) lists specific parameters that are used in simulation of semianalytical modeling. The results show they give lowest variation and probability of bit error. Thereby m, the system performance is optimized by increasing of SNR. The effect of the source chirp on the variance is also investigated in Fig. 1. It seems clear that the chirp increases the signal variance significantly. For long-haul transmission systems, the lowest value of chirping impact is shifted from positive to negative values. Also, for different values of dispersion parameters as compared with 4-QAM technique, the SNR for square M-QAM modulation techniques with high-order as 256-QAM is diminished to the threshold value in spite of the large amount of information transmitted through such systems. Figure 2 shows impact of initial Gaussian pulse-duration on the SNR. We checked out the impacts of peak power on the performance of square M-QAM system by checking out their impacts on SNR. For all square M-QAM transmitter systems, dispersion parameters at β_2 = -1 ps^2/km showed the least amount of variation. Based on the above results, we took into account the parameters listed in Table 2 as the approved parameters that reduce the effects of nonlinear distortion. In generally, the perturbation calculations contain infinite

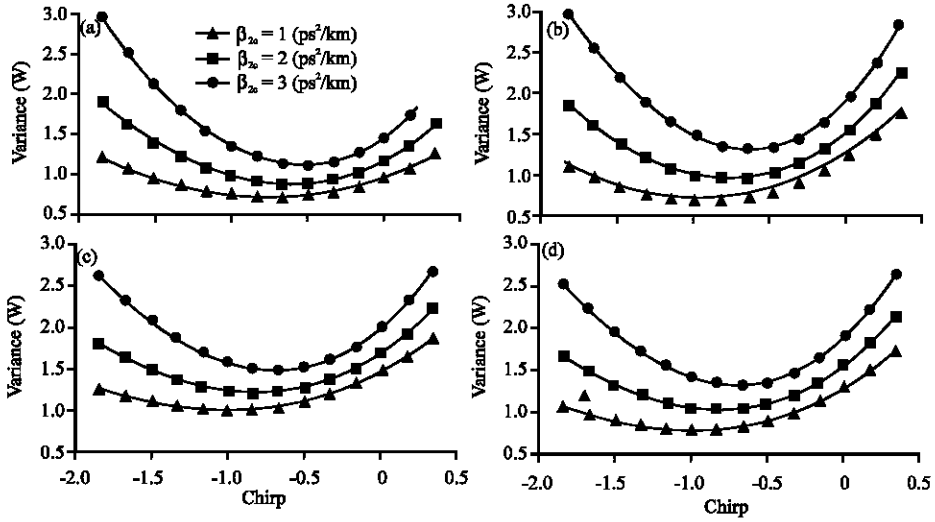

Fig. 1: Variance as a function of initial chirp for square M-QAM transmission techniques using different values of compensated dispersion per-span: a) 4-QAM; b) 16-QAM; c) 64-QAM and d) 256-QAM

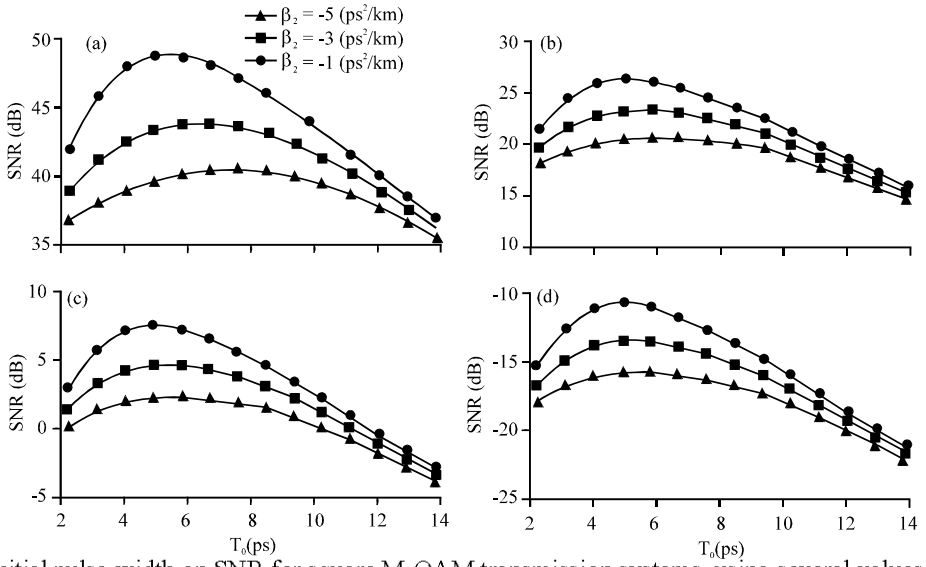

Fig. 2: Effect of initial pulse-width on SNR for square M-QAM transmission systems, using several values of dispersion per-span: a) 4-QAM; b) 16-QAM; c) 64-QAM and d) 256-QAM

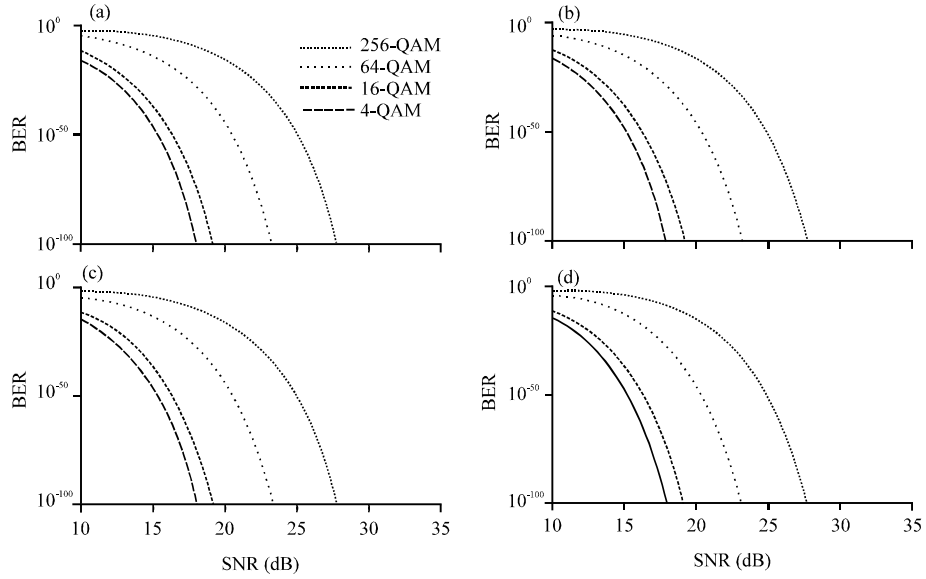

Fig. 3: Average BER versus SNR of a single-core fiber for M-QAM square transmission technique, using different values of source chirp. (amplifiedspontaneous emission noise is ignored): a) Chirp = -2; b) Chirp = -1; c) Chirp = 0 and c) Chirp = 1

terms when the approach be infinite. The computational complexity of the perturbation-based compensation scheme is proportional to the size of the coefficient matrix $\tilde{X}_{l,m,l+m}(\omega)$ and the number of summation terms (as shown in Eq. 11). Consequently, when the minimum SNR threshold is too low, the number of coefficients is not adequate to provide an accurate estimation of nonlinear distortion. In experimental implementations, to reduce the computational complexity, the insignificant components in the matrix $\tilde{X}_{l,m,l+m}(\omega)$ are truncated. For high-order M-QAM systems, we found that the BER is much higher than the threshold (A typical BER requirement is 10^{-12}-10^{-15} (Thyagarajan and Ghatak, 2007) due to the large transmission capacity of these systems. However, the result of such statistical tests is acceptable practically to interpret the data. Figure 3 shows BER as a function of SNR with different values of chirp. As can be seen, since the chirp of pulse has the same effect on both BER and SNR, there is no obvious impact on their relation. Also, the obtained SNR of square M-QAM which corresponds

Table 2: Simulation parameters for Gaussian pulses

Parameters	Values	Units
β_2	-1	ps^2/km
L	80	km
γ	1.1	W^{-1}/km
α	0.2	dB/km
T_b	25	ps
T_0	5	ps
P_0	0.1	mW
β_{2c}	1	ps^2/km
Chirp	-1	None
No. of span	12	None
No. of interacted signals (= 2s+1)	19	None

to BER.10^{-15} as follows: SNR8 dB for 4-QAM system, SNR = 9 dB for 16-QAM system, SNR = 13.5 dB for 64-QAM system, SNR = 19 dB for 256-QAM system. Compared with the previous studies of linear systems, the communication system is improved by selecting the best suitable parameters which greatly contribute to reducing the effects of intrachannel nonlinear distortions.

CONCLUSION

A semi-analytical Gaussian Model of intra-channel fiber nonlinearity impairments based on M-QAM square systems was developed. In order to mitigate the nonlinearity distortion using a first order perturbation technique, we proposed in this paper a significantly expression to reduce the computational time to estimate the BER. The total PSD and signal variance due to the nonlinear distortions were obtained, we found that the four types of intrachannel nonlinearity are the main involved sources of nonlinear distortion for the M-QAM square systems. The results showed by selecting suitable parameters, it is possible to optimize the fiber-optic communication system by reducing the intrachannel nonlinearity distortion increase the ratio of transmitted information and decrease the error rate to acceptable values.

ACKNOWLEDGEMENT

The researcher would like to thank Mustansiriyah University (www,uomustansiriyah,edu.iq) for their support in this research.

REFRENCES

Agrawal, G.P., 2012. Fiber-Optic Communication Systems. 4th Edn., John Wiley & Sons, Hoboken, New Jersey, USA., Pages: 2053.

Bononi, A., E. Grellier, P. Serena, N. Rossi and F. Vacondio, 2011. Modeling nonlinearity in coherent transmissions with dominant interpulse-four-wave-mixing. Proceedings of the 2011 37th European Conference and Exhibition on Optical Communication, September 18-22, 2015, IEEE, Geneva, Switzerland, ISBN:978-1-4577-1918-9, pp: 1-3.

Chen, T., K. Li, Y. Zuo and B. Zhu, 2015. QAM adaptive measurements feedback quantum receiver performance. J. Eng. Sci., 1: 1-6.

Cho, K. and D. Yoon, 2002. On the general BER expression of one-and two-dimensional amplitude modulations. IEEE. Trans. Commun., 50: 1074-1080.

Djordjevic, I.B. and B. Vasic, 2006. Constrained coding techniques for the suppression of intrachannel nonlinear effects in high-speed optical transmission. J. Lightwave Technol., 24: 411-419.

Gnauck, A.H., P.J. Winzer, A. Konczykowska, F. Jorge and J.Y. Dupuy, 2012. Generation and transmission of 21.4-Gbaud PDM 64-QAM using a novel high-power DAC driving a single I/Q modulator. J. Lightwave Technol., 30: 532-536.

Hirooka, T. and M. Nakazawa, 2015. Q-factor analysis of nonlinear impairments in ultrahigh-speed Nyquist pulse transmission. Opt. Express, 23: 33484-33492.

Jain, A. and R. Gupta, 2015. Gaussian filter threshold modulation for filtering flat and texture area of an image. Proceedings of the 2015 International Conference on Advances in Computer Engineering and Applications, March 19-20, 2015, IEEE, Ghaziabad, India, ISBN:978-1-4673-6911-4, pp: 760-763.

Kahn, J.M. and K.P. Ho, 2004. Spectral efficiency limits and modulation-detection techniques for DWDM systems. IEEE. J. Sel. Top. Quantum Electron., 10: 259-272.

Kato, K., 2012. Error performance of quantum minimax receiver for 16QAM overlapping states signal. Tamagawa Univ. Quantum ICT. Res. Inst. Bull., 2: 19-24.

Liang, X., 2015. Analysis and compensation of nonlinear impairments in fiber-optic communication systems. Ph.D Thesis, McMaster University, Hamilton, Canada.

Lopes, W.T.A., W.J.L. Queiroz, F. Madeiro and M.S. Alencar, 2007. Exact bit error probability of M-QAM modulation over flat Rayleigh fading channels. Proceedings of the 2007 SBMO/IEEE MTT-S International Conference on Microwave and Optoelectronics Conference, October 29- November 1, 2007, IEEE, Brazil, South America, ISBN:978-1-4244-0660-9, pp: 804-806.

Naderi, S.S., 2013. Analysis and mitigation of the nonlinear impairments in fiber-optic communication systems. Ph.D Thesis, University of Waterloo, Waterloo, Canada.

Schmidt, J.F., U. Schilcher and C. Bettstetter, 2016. Exact bit error rate expressions for interference-limited Poisson networks. Electron. Lett., 52: 1961-1963.

Shake, I., H. Takara, K. Mori, S. Kawanishi and Y. Yamabayashi, 1998. Influence of inter-bit four-wave mixing in optical TDM transmission. Electron. Lett., 34: 1600-1601.

Tao, Z., Y. Zhao, Y. Fan, L. Dou and T. Hoshida *et al*., 2015. Analytical intrachannel nonlinear models to predict the nonlinear noise waveform. J. Lightwave Technol., 33: 2111-2119.

Thyagarajan, K.S. and A. Ghatak, 2007. Fiber Optic Essentials. John Wiley and Sons Inc., New Jersey, ISBN-13: 9780470152553, Pages: 344.

Wang, M., S. Zheng, X. Li and X. Qin, 2014. A new image denoising method based on Gaussian filter. Proceedings of the 2014 International Conference on Information Science, Electronics and Electrical Engineering, April 26-28, 2014, IEEE, Sapporo, Japan, ISBN:978-1-4799-3196-5, pp: 163-167.

Zhang, J., S. Zhang and J. Wang, 2017. Pseudorange measurement method based on AIS signals. Sens., 17: 1-20.